# SURFACE PHYSICS

A.V. KOROTUN, YA.V. KARANDAS'

National University "Zaporizhzhia Politechnic"
*(64, Zhukovs'kogo Str., Zaporizhzhya 69063, Ukraine; e-mail: andko@zntu.edu.ua)*

# ENERGY CHARACTERISTICS OF METAL NANOWIRES WITH PERIODICALLY MODULATED SURFACE

*The energy spectrum of electrons in a metal nanowire with a periodically modulated surface has been found in the framework of perturbation theory. To solve the problem, a transition is made into a coordinate system that "smoothes down" the surface oscillations. The influence of the surface modulation amplitude on size-induced oscillations of the Fermi energy in such systems is analyzed. It is shown that an increase of the modulation amplitude leads to a decrease of the Fermi energy in the wire. Specific calculations were made for Au, Cu, and Al wires.*

*K e y w o r d s: nanowire, Fermi energy, modulation amplitude, perturbation theory.*

## 1. Introduction

The development of nanotechnology gave rise to the synthesis and applications of metal nanostructures with various configurations and, accordingly, different optical properties. Among such objects, structures that have nanometer sizes in two directions–they are called metal nanoconductors–occupy a special place [1–9]. Interest in the study of the properties of 1D systems is associated with their widespread applications in nanophotonics (in particular, as elements of optical antennas [10, 11]), spectroscopy (in order to increase the Raman screening cross-section [12]), and single-molecule fluorescence spectroscopy [13], as well as probes for near-field optical microscopy [14] and components of lasers, biosensors, and other devices [15].

When fabricating the metal nanowires, the influence of mechanical stresses that vary along the wire length may lead to a deviation of the wire surface shape from the cylindrical one. The most common cases of distorting the wire surface are the stochastic relief and the periodic modulation along the nanowire axis. The latter case, in particular, may be related to the crystalline structure of a wire near its surface, when the potential field at the nanowire surface becomes a periodic function of the longitudinal coordinate. Furthermore, the choice of a periodic relief is explained by its analogy with the case of nanofilms, for which it was experimentally confirmed that the surface shape is close to periodic [16].

The optical properties of systems with a reduced dimensionality are determined to a large extent by the excitation of their electron subsystem. One of the most important parameters of this subsystem is the Fermi energy. Its dependence on the specimen sizes is responsible for the oscillations of such optical characteristics of nanostructures as the optical conductivity, dielectric function, and absorption coefficient [17–19].

The authors of works [6, 20, 21] considered the electronic properties of charge carriers in nanowires with a random surface relief. In particular, the charge carrier scattering by heterogeneities at the metal nanowire surface was analyzed in work [20], the scattering at interface inhomogeneities and the electron mobility in quantum wires in work [20], and the scattering on inhomogeneities induced by the insulator-metal-insulator transition in work [21]. The energy spectrum of charge carriers in 1D systems with pe-

riodically modulated surface was obtained in work [22]. However, the issue about the effect of the periodic surface modulation on the behavior of the Fermi energy in metal nanowires still remains unexplored and, therefore, challenging.

## 2. Formulation of the Problem and Basic Relations

The lateral surface of a nanowire with a circular cross-section and a periodic, along the wire length, surface relief is given in the polar coordinate system by the equation $\rho = \rho_0 + f(z)$, where $f(z) = a\cos\varkappa z$ is a periodic function with the spatial period $\Lambda = 2\pi/\varkappa$, $\rho_0 = \text{const}$ is the average wire radius, $a$ is the surface modulation depth $(a \ll \rho_0)$, and the $z$ axis is directed along the wire axis. Let us change to a new coordinate system:

$$\rho' = \frac{\rho_0 \rho}{\rho_0 + f(z)}, \quad \varphi' = \varphi, \quad z' = z,$$

in which the conductor surface is cylindrical and described by the equation $\rho' = \rho_0$. Then, the Laplace operator in the Schrödinger equation is transformed according to the formula

$$\Delta = \frac{1}{\sqrt{g}} \sum_{i,k} \partial_i \left(\sqrt{g}\, g^{ik} \partial_k\right), \tag{1}$$

where $g = \det\left[\left(g^{ik}\right)^{-1}\right]$, and $g^{ik}$ is a contravariant metric tensor, whose components are determined by the expression [23]

$$g^{ik}(\rho', \varphi', z') = \frac{\partial x_i}{\partial \rho}\frac{\partial x_k}{\partial \rho} + \frac{\partial x_i}{\partial \varphi}\frac{\partial x_k}{\partial \varphi} + \frac{\partial x_i}{\partial z}\frac{\partial x_k}{\partial z}, \quad (2)$$
$$x_{i,k} = \rho', \varphi', z'.$$

Calculating all components of this tensor (see Appendix A), we obtain

$$g^{ik} = \begin{pmatrix} \dfrac{\rho'^2 f'^2_{z'} + \rho_0{}^2}{(\rho_0 + f(z'))^2} & 0 & -\dfrac{\rho' f'_{z'}}{\rho_0 + f(z')} \\ 0 & \dfrac{\rho_0{}^2}{\rho'^2(\rho_0 + f(z'))^2} & 0 \\ -\dfrac{\rho' f'_{z'}}{\rho_0 + f(z')} & 0 & 1 \end{pmatrix},$$
$$\sqrt{g} = \frac{\rho'(\rho_0 + f(z'))^2}{\rho_0{}^2}. \tag{3}$$

Hence, in new coordinates, the Laplace operator looks like

$$\Delta = \frac{\rho_0{}^2 + \rho'^2 f'^2_{z'}}{(\rho_0 + f(z'))^2}\frac{\partial^2}{\partial\rho'^2} + \frac{\rho_0{}^2 + \rho'^2 f'^2_{z'}}{(\rho_0 + f(z'))^2}\frac{1}{\rho'}\frac{\partial}{\partial\rho'} +$$
$$+ \frac{\rho' f'^2_{z'}}{(\rho_0 + f(z'))^2}\frac{\partial}{\partial\rho'} - \frac{2\rho' f'_{z'}}{\rho_0 + f(z')}\frac{\partial}{\partial\rho'\partial z'} -$$
$$- \frac{\rho' f''_{z'z'}}{\rho_0 + f(z')}\frac{\partial}{\partial\rho'} + \frac{\partial^2}{\partial z'^2}, \tag{4}$$

where the notations

$$f'_{z'} \equiv \frac{df(z')}{dz'}, \quad f''_{z'z'} \equiv \frac{d^2 f(z')}{dz'^2} \tag{5}$$

were introduced. In the applied approximation, $\max f'_{z'} = a\varkappa \ll 1$, $\max(a f''_{z'z'}) = a^2\varkappa^2 \ll 1$, and $\rho' f'_{z'} \ll \rho_0$. Therefore, in the first order of perturbation theory in the quantity $a/\rho_0$, the Laplace operator is described by the expression

$$\Delta \cong \frac{\rho_0{}^2}{(\rho_0 + f(z'))^2}\left(\frac{\partial^2}{\partial\rho'^2} + \frac{1}{\rho'}\frac{\partial}{\partial\rho'}\right) + \frac{\partial^2}{\partial z'^2}.$$

The surface modulation amplitude is considered to be small in comparison with the average nanowire radius $(a/\rho_0 \ll 1)$. Then, according to perturbation theory, the Hamiltonian has the form

$$\hat{\mathcal{H}} = \hat{\mathcal{H}}_0 + \hat{V},$$

or

$$\hat{\mathcal{H}} = -\frac{\hbar^2}{2m_e} \times$$
$$\times \left[\frac{\rho_0^2}{(\rho_0 + f(z'))^2}\left(\frac{\partial^2}{\partial\rho'^2} + \frac{1}{\rho'}\frac{\partial}{\partial\rho'} + \frac{1}{\rho'}\frac{\partial^2}{\partial\varphi'^2}\right) + \frac{\partial^2}{\partial z'^2}\right].$$

The Hamiltonian of the unperturbed problem looks like

$$\hat{\mathcal{H}}_0 = -\frac{\hbar^2}{2m_e}\left[\frac{\partial^2}{\partial\rho'^2} + \frac{1}{\rho'}\frac{\partial}{\partial\rho'} + \frac{1}{\rho'^2}\frac{\partial^2}{\partial\varphi'^2} + \frac{\partial^2}{\partial z'^2}\right],$$

and its eigenvalues equal

$$E_{mn}^{(0)} = \frac{\hbar^2 k_{mn}^{(0)2}}{2m_e}.$$

The perturbation operator has the form (see Appendix B)

$$\hat{V} = \frac{\hbar^2}{m_e}\frac{a}{\rho_0}\left(\frac{\partial^2}{\partial\rho'^2} + \frac{1}{\rho'}\frac{\partial}{\partial\rho'} + \frac{1}{\rho'^2}\frac{\partial^2}{\partial\varphi'^2}\right)\cos\varkappa z'. \tag{6}$$

The first-order correction to the spectrum is determined by the expression

$$E_{mn}^{(1)} = \frac{\hbar^2 k_{mn}^{(0)} k_{mn}^{(1)}}{m_e} \qquad (7)$$

or

$$E_{mn}^{(1)} = \int_{V'} \psi_{mnp}^{(0)*} (\rho', \varphi', z') \, \hat{V} \psi_{mnp}^{(0)} (\rho', \varphi', z') \, dV'. \qquad (8)$$

In the zeroth approximation, we select the wave functions for a circular wire in the form [18]

$$\psi_{mnp}^{(0)} (\rho', \varphi', z') = R_{mn} (\rho') \, \Phi_m (\varphi') \, Z_p (z'),$$

where

$$Z_p (z') = \frac{1}{\sqrt{L}} \, e^{-ik_{z'p} z'}$$

is a part of the wave function that corresponds to the longitudinal motion of an electron along the axis of the wire with the length $L$, the subscript $p$ enumerates the values of the $z$-component of the wave vector,

$$\Phi_m (\varphi') = \frac{1}{\sqrt{2\pi}} \, e^{-im\varphi'}$$

is the angular part of the wave function ($m = 0.1, ...$),

$$R_{mn} (\rho') = C_{mn} I_m (k_{mn} \rho')$$

is the radial part of the wave function, and

$$C_{mn} = \frac{\sqrt{2}}{\rho_0' \left| I_m' \left( k_{mn}^{(0)} \rho_0 \right) \right|}.$$

The calculation of integral (8) making use of Eq. (7) results in the following correction to the wave number:

$$k_{mn}^{(1)} = 2k_{mn}^{(0)} \frac{a}{\rho_0} \frac{\sin \varkappa L}{\varkappa L}. \qquad (9)$$

In the zeroth order of perturbation theory, the spectrum is determined from the transcendental equation [24]

$$k_{mn}^{(0)} \frac{I_m' \left( k_{mn}^{(0)} \rho_0 \right)}{I_m \left( k_{mn}^{(0)} \rho_0 \right)} = \varkappa_{mn}^{(0)} \frac{K_m' \left( \varkappa_{mn}^{(0)} \rho_0 \right)}{K_m \left( \varkappa_{mn}^{(0)} \rho_0 \right)}, \qquad (10)$$

where $I_m (x)$, $K_m (x)$, $I_m' (x)$, and $K_m' (x)$ are the Bessel and MacDonald functions of the $m$-th order and their first derivatives, respectively; $\varkappa_{mn}^{(0)\,2} =$

$= k_0^2 - k_{mn}^{(0)\,2}$; $\hbar k_0 = \sqrt{2m_e U_0}$; and $U_0$ is the potential well depth. Making allowance for the first-order correction, the spectrum looks like

$$k_{mn} \cong k_{mn}^{(0)} + k_{mn}^{(1)} = k_{mn}^{(0)} \left( 1 + 2\frac{a}{\rho_0} \frac{\sin \varkappa L}{\varkappa L} \right). \qquad (11)$$

In the same approximation, the eigenvalues of the Hamiltonian equal

$$E_{mn} = \frac{\hbar^2 k_{mn}^2}{2m_e} = \frac{\hbar^2 k_{mn}^{(0)2}}{2m_e} \left( 1 + 2\frac{a}{\rho_0} \frac{\sin \varkappa L}{\varkappa L} \right)^2 \cong$$

$$\cong \frac{\hbar^2 k_{mn}^{(0)2}}{2m_e} \left( 1 + 4\frac{a}{\rho_0} \frac{\sin \varkappa L}{\varkappa L} \right).$$

Since the surface modulation is considered to take place on a large scale ($2\pi/\varkappa \gg 1$), it follows that $\varkappa L \ll 1$. In this case, $\sin \varkappa L / \varkappa L \cong 1$ with a sufficient accuracy, and we may write that

$$E_{mn} \cong \frac{\hbar^2 k_{mn}^{(0)2}}{2m_e} \left( 1 + 4\frac{a}{\rho_0} \right). \qquad (12)$$

The second term in parentheses determines a correction to the spectrum caused by the periodic modulation of the wire surface.

The size dependence of the Fermi energy is determined by the relation [18]

$$\bar{n} = \frac{2}{\pi^2 \rho_0^2} \sum_{m,n} \sqrt{k_{\mathrm{F}}^2 - k_{mn}^2}, \qquad (13)$$

where $\bar{n}$ is the concentration of conduction electrons in the 3D metal, and the numbers $k_{mn}$ are determined from Eq. (11). In formula (13), the summation is carried out over all $m$ and $n$ values, for which $k_{mn} < k_{\mathrm{F}}$.

## 3. Calculation Results and Their Discussion

Specific calculations were performed for Al ($Z = 3$), Cu ($Z = 2$), and Au ($Z = 1$) nanoconductors with the electron concentration $\bar{n} = 3/4\pi r_s^3$ determined for corresponding values $r_s = 2.07a_0$, $2.11a_0$, and $3.01a_0$, respectively. Here, $Z$ is the metal valence, $r_s$ the average distance between electrons, and $a_0$ the Bohr radius. The modulation amplitude was taken to equal $a/\rho_0 = 0$, 0.05, and 0.1. The nanowires were supposed to be embedded into $SiO_2$ (the depth of the conduction band bottom with respect to the vacuum

level, i.e. the electron affinity, $\chi = 1.1$ eV, and the dielectric constant $\epsilon = 4$) or $Al_2O_3$ ($\chi = 1.35$ eV, $\epsilon = 9$) [25].

For the band structure of the insulator [26] to be taken into account, it is necessary to redetermine the work function of electrons from the nanowire and, hence, the well depth. Unlike the case of a wire in vacuum, where

$$U_0 = \varepsilon_F^0 + W_0,$$

the presence of an insulator results in a decrease of the work function and the well depth $U_d$ from the insulator side,

$$U_d = \varepsilon_F^0 + W_d,$$

where $W_d$ is the potential barrier height at the metal-insulator interface (Schottky barrier).

By analogy with work [26], let us take advantage of two approaches to the determination of $W_d$:

(I) the work function into the insulator is determined as the difference $W_d = W_0 - \chi$, where $W_0$ is the work function at the interface semiinfinite metal–vacuum;

(II) the value of $W_d$ is taken from the results of self-consistent calculations (see Table).

The results of calculations of the size dependence of the Fermi energy $\varepsilon_F$ (in the relative units $\varepsilon_F/\varepsilon_F^0$, where $\varepsilon_F^0 = \hbar^2 \left(3\pi^2 \bar{n}\right)^{\frac{2}{3}}/(2m_e)$ is the Fermi energy in a uniform electron gas) carried out in the framework of those two approaches for an Au nanowire in the $Al_2O_3$ and $SiO_2$ media and for the modulation amplitude $a/\rho_0 = 0.1$ are shown in Fig. 1 (panels $a$ and $b$, respectively). Curves 1 correspond to approach I, and curves 2 to approach II. For both approaches, the results are qualitatively similar. Namely, the characters of the dependences for both insulators are similar, and,, for both dependences, there is a significant reduction of the oscillation amplitude with the growth of the effective nanowire diameter. However, they differ quantitatively in both the amplitude (by about 5–7%) and the position of the peaks: $\max\left(\varepsilon_F/\varepsilon_F^0\right)_I < \max\left(\varepsilon_F/\varepsilon_F^0\right)_{II}$, i.e., the maxima in approach I are shifted to the left with respect to the maxima in approach II because of the difference between the values of the potential well depth.

The results of self-consistent calculations are more correct, because, unlike approach I, where the work
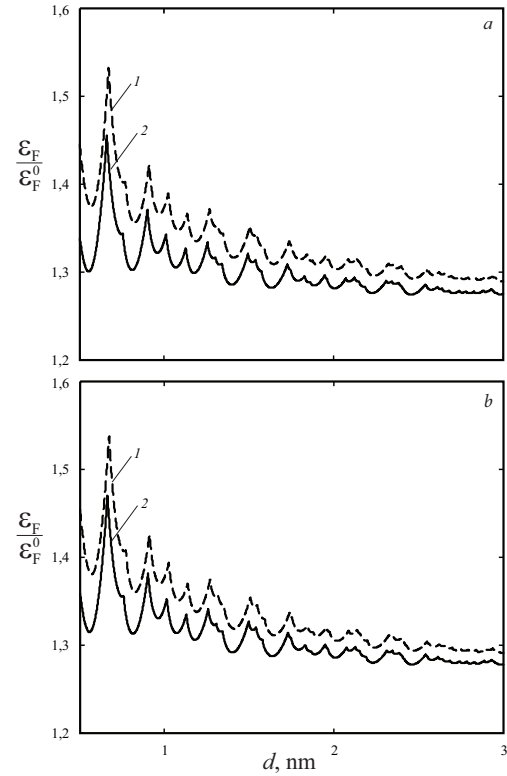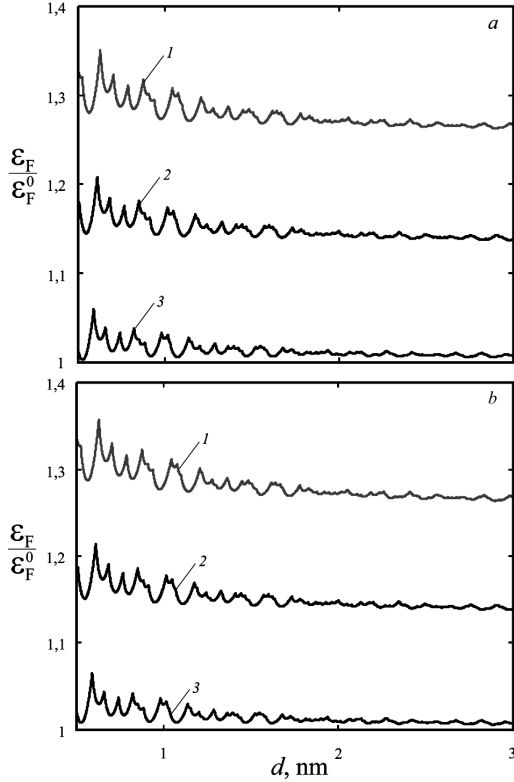


**Fig. 1.** Size dependences of the Fermi energy for an Au nanowire in the $Al_2O_3$ ($a$) and $SiO_2$ ($b$) media. $d = 2\rho_0$

**Results of self-consistent calculations for semiconfined systems**

| Metal | Al | | Cu | | Au | |
|---|---|---|---|---|---|---|
| Insulator | $Al_2O_3$ | $SiO_2$ | $Al_2O_3$ | $SiO_2$ | $Al_2O_3$ | $SiO_2$ |
| $W_d$, eB | 1.29 | 1.84 | 1.49 | 1.89 | 1.41 | 1.79 |

function into the insulator is a given parameter, this value is calculated by solving together the Schrödinger and Poisson equations, i.e., the charge redistribution is taken into account. In this connection, approach II will be used below.

Figure 2 demonstrates the size dependences of the ratio $\varepsilon_F/\varepsilon_F^0$ for Cu nanowires in various dielectric media and at various modulation amplitude values. One can see that, as the parameter $a/\rho_0$ increases, the $\varepsilon_F/\varepsilon_F^0$-values decrease, and the peaks in the size dependences insignificantly move to the right, which is associated with the variation of the effective potential well width.

**Fig. 2.** Size dependences of the Fermi energy for a Cu nanowire in the $Al_2O_3$ (*a*) and $SiO_2$ (*b*) media at various modulation amplitudes $a/\rho_0 = 0$ (*1*), 0.05 (*2*), and 0.1 (*3*). $d = 2\rho_0$
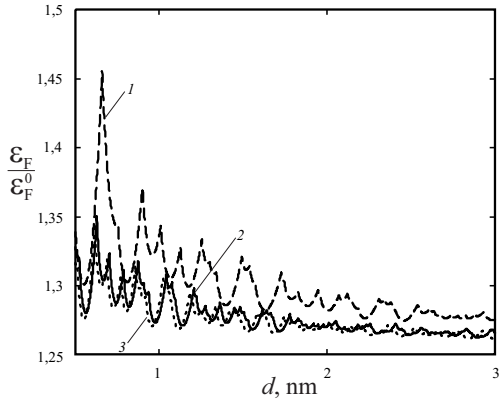


**Fig. 3.** Size dependences of the Fermi energy for nanowires of various metals in the $SiO_2$ medium at $a/\rho_0 = 0.1$: Au (*1*), Cu (*2*), and Al (*3*). $d = 2\rho_0$

Analogous dependences for various metals but at the fixed modulation amplitude ($a/\rho_0 = 0.1$) are shown in Fig. 3. A substantial difference between the quantitative results obtained for Au nanowires and

the closeness of the results for Cu and Al ones can be exhaustively explained by the values of the parameter $r_s$ for those metals.

## 4. Conclusions

In this work, the issue how periodic modulations of the surface of metal nanowires affect the size dependence of the Fermi energy in the conductor has been considered. The oscillations in this dependence determine the behavior of the optical characteristics of 1D systems.

In the framework of two approaches, the size-induced oscillations of the Fermi energy are calculated for Al, Cu, and Au conductors in various dielectric media and at various surface modulation amplitudes. It is found that, for an Au nanowire in the $Al_2O_3$ and $SiO_2$ media, the both approaches give qualitatively similar results for the modulation amplitude $a/\rho_0 = 0.1$. However, those results differ quantitatively in the oscillation amplitude and the peak positions owing to different potential well depths.

By the example of a Cu nanowire, it is demonstrated that the relative values of the Fermi energy decrease with the modulation amplitude growth. This result is explained by the fact that the modulation amplitude growth leads to a potential well deformation and changes its effective width, so that the Fermi level decreases.

At fixed modulation amplitudes, the results of calculations are close quantitatively for the Cu and Al nanowires, but differ significantly for the Au one. This is a result of the closeness of the $r_s$-values for the first two metals and their significant difference with the case of Au.

**APPENDIX A.**
**Calculation of the Components**
**of the Contravariant Metric Tensor**

Let us calculate the components of the contravariant metric tensor using formula (2):

$$g^{11} = \left(\frac{\partial \rho'}{\partial \rho}\right)^2 + \frac{1}{\rho^2}\left(\frac{\partial \rho'}{\partial \varphi}\right)^2 + \left(\frac{\partial \rho'}{\partial z}\right)^2 =$$

$$= \frac{\rho_0^2}{(\rho_0 + f(z'))^2} + \frac{\rho_0^2 \rho^2 f_z'^2}{(\rho_0 + f(z'))^4} = \frac{\rho'^2 f_{z'}'^2 + \rho_0^2}{(\rho_0 + f(z'))^2};$$

$$g^{22} = \left(\frac{\partial \varphi'}{\partial \rho}\right)^2 + \frac{1}{\rho^2}\left(\frac{\partial \varphi'}{\partial \varphi}\right)^2 + \left(\frac{\partial \varphi'}{\partial z}\right)^2 =$$

$$= \frac{1}{\rho^2} = \frac{\rho_0{}^2}{\rho'^2 (\rho_0 + f(z'))^2};$$

$$g^{33} = \left(\frac{\partial z'}{\partial \rho}\right)^2 + \frac{1}{\rho^2}\left(\frac{\partial z'}{\partial \varphi}\right)^2 + \left(\frac{\partial z'}{\partial z}\right)^2 = 1,$$

$$g^{12} = g^{21} = \rho\frac{\partial \rho'}{\partial \rho}\frac{\partial \varphi'}{\partial \rho} + \frac{1}{\rho}\frac{\partial \rho'}{\partial \varphi}\frac{\partial \varphi'}{\partial \varphi} + \rho\frac{\partial \rho'}{\partial z}\frac{\partial \varphi'}{\partial z} = 0,$$

$$g^{23} = g^{32} = \rho\frac{\partial \varphi'}{\partial \rho}\frac{\partial z'}{\partial \rho} + \frac{1}{\rho}\frac{\partial \varphi'}{\partial \varphi}\frac{\partial z'}{\partial \varphi} + \rho\frac{\partial \varphi'}{\partial z}\frac{\partial z'}{\partial z} = 0,$$

$$g^{13} = g^{31} = \rho\frac{\partial \rho'}{\partial \rho}\frac{\partial z'}{\partial \rho} + \frac{1}{\rho}\frac{\partial \rho'}{\partial \varphi}\frac{\partial z'}{\partial \varphi} + \rho\frac{\partial \rho'}{\partial z}\frac{\partial z'}{\partial z} =$$

$$= -\frac{\rho_0 f'(z)\rho}{(\rho_0 + f(z))^2} = -\frac{\rho' f'_{z'}}{\rho_0 + f(z')}.$$

Relation (3) follows from the formulas given above.

## APPENDIX B. Perturbation operator

Let us define the perturbation operator:

$$\hat{V} = \hat{\mathcal{H}} - \hat{\mathcal{H}}_0 = -\frac{\hbar^2}{2m_e} \times$$

$$\times \left(\frac{\rho_0^2}{(\rho_0 + f(z'))^2} - 1\right)\left(\frac{\partial^2}{\partial \rho'^2} + \frac{1}{\rho'}\frac{\partial}{\partial \rho'} + \frac{1}{\rho'^2}\frac{\partial^2}{\partial \varphi'^2}\right) =$$

$$= -\frac{\hbar^2}{2m_e}\frac{\rho_0^2 - (\rho_0 + f(z'))^2}{(\rho_0 + f(z'))^2} \times$$

$$\times \left(\frac{\partial^2}{\partial \rho'^2} + \frac{1}{\rho'}\frac{\partial}{\partial \rho'} + \frac{1}{\rho'^2}\frac{\partial^2}{\partial \varphi'^2}\right) =$$

$$= -\frac{\hbar^2}{2m_e}\frac{\rho_0^2 - \rho_0^2 - 2\rho_0 f(z') - f^2(z')}{\rho_0^2 + 2pf(z') + f^2(z')} \times$$

$$\times \left(\frac{\partial^2}{\partial \rho'^2} + \frac{1}{\rho'}\frac{\partial}{\partial \rho'} + \frac{1}{\rho'^2}\frac{\partial^2}{\partial \varphi'^2}\right) =$$

$$= \frac{\hbar^2}{2m_e}\frac{2\frac{a}{\rho_0}\cos \varkappa z' + \frac{a^2}{\rho_0^2}\cos^2 \varkappa z'}{1 + 2\frac{a}{\rho_0}\cos \varkappa z' + \frac{a^2}{\rho_0^2}\cos^2 \varkappa z'} \times$$

$$\times \left(\frac{\partial^2}{\partial \rho'^2} + \frac{1}{\rho'}\frac{\partial}{\partial \rho'} + \frac{1}{\rho'^2}\frac{\partial^2}{\partial \varphi'^2}\right) \cong$$

$$\cong \frac{\hbar^2}{m_e}\frac{a}{\rho_0}\left(\frac{\partial^2}{\partial \rho'^2} + \frac{1}{\rho'}\frac{\partial}{\partial \rho'} + \frac{1}{\rho'^2}\frac{\partial^2}{\partial \varphi'^2}\right)\cos \varkappa z'.$$

From whence, formula (6) is obtained.

1. P.M. Tomchuk. Oscillations of optical conductivity and emission in quantum metal conductors. *Ukr. Fiz. Zh.* **47**, 833 (2002) (in Ukrainian).
2. Al. Moroz. Electron mean-free path in metal-coated nanowires. *J. Opt. Soc. Am. B* **28**, 1130 (2011).
3. H.L. Chen, L. Gao. Anomalous electromagnetic scattering from radially anisotropic nanowires. *Phys. Rev. A* **86**, 033825 (2012).
4. St. H. Simpson, P. Zemanek, O.M. Marago, Ph.H. Jones, S. Hanna. Optical binding of nanowires. *Nano Lett.* **17**, 3485 (2017).
5. L. Zhang, Yi Zhou, X. Dai, Zh. Zhao, H. Li. Electronic transport properties of lead nanowires. *Chin. Phys. B* **26**, 073102 (2017).
6. Kr. Moors, B. Soree, W. Magnus. Modeling surface roughness scattering in metallic nanowires. *J. Appl. Phys* **118**, 124307 (2015).
7. M. Michailov, D. Kashchiev. Monatomic metal nanowires: Rupture kinetics and mean lifetime. *Phys. E* **70**, 21 (2015).
8. P. Cui, J-H. Choi, H. Lan, J-H. Cho, Q. Niu, J. Yang, Zh. Zhang. Quantum stability and magic lengths of metal atom wires. *Phys. Rev. B* **93**, 224102 (2016).
9. Zh. He, Zh. Zhou. Theoretically analyzed optical property of silver nanowire on a SiO$_2$ layer. *IEEE Photon. J.* **10**, 2856856 (2018).
10. A. Pucci, F. Neubrech, D. Weber, S. Hong, T. Toury, M. Lamy de la Chapelle. Surface enhanced infrared spectroscopy using gold nanoantennas. *Phys. Status Solidi B* **247**, 2071 (2010).
11. D.A. Zuev, S.V. Makarov, I.S. Mukhin, S.V. Starikov, I.A. Morozov, I.I. Shishkin, A.E. Krasnok, P.A. Belov. Fabrication of Hybrid Nanostructures via Nanoscale Laser-Induced Reshaping for Advanced Light Manipulation [*eprint arXiv:1601.02013*].
12. M. Fan, G.F. Andrade, A.G. Brolo. A review on the fabrication of substrates for surface enhanced Raman spectroscopy and their applications in analytical chemistry. *Anal. Chim. Acta* **693**, 7 (2011).
13. J. Dorfmüller, R. Vogelgesang, W. Khunsin, C. Rockstuhl, C. Etrich, K. Kern. Plasmonic nanowire antennas: experiment, simulation, and theory. *Nano Lett.* **10**, 3596 (2010).
14. T.H. Taminiau, F.D. Stefani, F.B. Segerink, N.F. van Hulst. Optical antennas direct single-molecule emission. *Nat. Photon.* **2**, 234 (2008).
15. E.A. Velichko, A.P. Nikolaenko. Nanocylinders from noble metal as diffusers of plane electromagnetic wave. *Radiofiz. Elektron.* **20**, 62 (2015) (in Russian).
16. Y. Namba, J. Yu, J.M. Bennett, K. Yamashita. Modeling and measurements of atomic surface roughness. *Appl. Opt.* **39**, 2705 (2000).
17. V.P. Kurbatskyi, A.V. Korotun, V.V. Pogosov. Optical conductivity and absorption of thin metal films in the infra-red spectral range. *Ukr. Fiz. Zh.* **53**, 569 (2008) (in Ukrainian).
18. V.P. Kurbatskii, A.V. Korotun, A.V. Babich, V.V. Pogosov. Fermi energy and optical conductivity of quantum metal filaments. *Fiz. Tverd. Tela* **51**, 2371 (2009) (in Russian).
19. A.V. Korotun, V.P. Kurbatskii, V.V. Pogosov. Dielectric function of 1D metal systems. *Zh. Nano Elektron. Fiz.* **8**, 04070 (2016) (in Russian).
20. J. Motohisa, H. Sakaki. Interface roughness scattering and electron mobility in quantum wires. *Appl. Phys. Lett.* **60**, 1315 (1992).
21. H. Fu, M. Sammon, B.I. Shklovskii. Roughness scattering induced insulator-metal-insulator transition in a quantum wire. *Phys. Rev. B* **97**, 035304 (2018).

22. V.I. Konchenkov, S.V. Kryuchkov. Electronic states in a quantum wire with the circular cross section and a periodically modulated surface. *Izv. Volg. Gos. Tekh. Univ.* **2**, 31 (2008) (in Russian).

23. G.A. Korn, T.M. Korn. *Mathematical Handbook for Scientists and Engineers* (McGraw-Hill, 1968).

24. A.V. Korotun, A.A. Koval. On the influence of insulator on the Fermi energy oscillations in an elliptic metal nanowire. *Fiz. Tverd. Tela* **57**, 1813 (2015) (in Russian).

25. E.H. Rhoderick. *Metal–Semiconductor Contacts* (Clarendon Press, 1978).

26. A.V. Korotun, Ya.V. Karandas. Energy characteristics of a metal nanofilm in a dielectric environment. *Zh. Nano Elektron. Fiz.* **7**, 02018 (2015) (in Ukrainian).

*А.В. Коротун, Я.В. Карандасъ*

ЕНЕРГЕТИЧНІ ХАРАКТЕРИСТИКИ
МЕТАЛЕВИХ НАНОДРОТІВ З ПЕРІОДИЧНО
МОДУЛЬОВАНОЮ ПОВЕРХНЕЮ

Р е з ю м е

З використанням теорії збурень знайдено енергетичний спектр електронів у металевому нанодроті з періодично модульованою поверхнею. Для розв'язку поставленої задачі було здійснено перехід у систему координат, що "спрямляє" межі. Досліджено вплив амплітуди модуляції на розмірні осциляції енергії Фермі таких систем. Показано, що збільшення амплітуди модуляції приводить до зменшення енергії Фермі дроту. Розрахунки було проведено для дротів Au, Cu та Al.